Generalized Molecular Orbital Theory II

Marc Couty[†] and Michael B. Hall*

Department of Chemistry, Texas A&M University, College Station, Texas 77843-3255

Received: December 3, 1996; In Final Form: June 27, 1997[⊗]

The generalized molecular orbital (GMO) concept is extended to a higher order method, which begins with a pair-excited multiconfiguration self-consistent field (PEMCSCF) for the orbital optimization and is followed by a multireference configuration interaction calculation. Here, this method is referred to as GMO2. The method has the advantage of being variational, of handling large numbers of active electrons, and of only needing the user to specify the number of active electrons and orbitals without specifying a dominant MO or VB configuration. In this paper, we briefly review the PEMCSCF theory, describe in more detail a new and more efficient optimization procedure, and propose determining the energy with configuration interaction (CI) at the single, double, triple, and quadruple-excitation levels (SDTQ) as a replacement for the full CI, which is needed in a complete active space (CAS) method. Several examples of the application of the method are investigated: methane, tetrahydrogen, benzene, dinitrogen dissociation, acetylene dissociation. For the five systems studied, the PEMCSCF orbital optimization produces orbitals that only differ from those of a CASSCF by an average of 4 kcal/mol when both localized bond type or symmetry-adapted orbitals are used in a full CI, GMO2(FCI). The additional error of replacing full CI with a SDTQ CI, GMO2(SDTQ), is usually less than 1 kcal/mol.

Introduction

Suitable *ab initio* methods to calculate the electronic structure of large molecules with significant multireference character, as found in many transition metal systems, are generally lacking. Often the closest Hartree−Fock approximation[1] to the ground state is triplet and/or singlet unstable. When this problem is severe, it can eliminate Moller−Plesset perturbation methods[2] as suitable solutions to the correlation problem. It can also eliminate coupled cluster methods, such as QCISD(T)[3] and CCSD(T),[4] which are based on a single reference as suitable approximations. Thus, for these cases, one is forced to rely on variational methods. Simple configuration interaction procedures such as CISD[5] may be unsuitable because of lack of size consistency. One is left with multiconfiguration self-consistent field methods (MCSCF[6], CASSCF[7], GVB,[8] spin-coupled VB[9]), usually followed by multireference configuration interaction (MRCI[10]) or by perturbation approximations to the MRCI (CASPT2[11]). For many systems, especially metal complexes and metal dimer complexes, the number of active electrons is simply too large for a full CASSCF calculation. Although the GVB approximation offers a viable alternative in some situations, it may be difficult to apply in practice when no single VB reference structure dominates.

Our original generalized molecular orbital[12] (GMO1) procedure was developed to overcome many of these deficiencies. However, it was limited by needing to specify a dominant single determinant. For many systems with multiple bonds, the wave function is not dominated by a single determinant. In particular, metal dimers often have several electronic configurations of the same overall symmetry that are nearly degenerate.[13] For these problems in both metal and nonmetal systems, one would like a method with the following characteristics:

1. The method must be variational (satisfied by CASSCF, GVB, and MRCI but not by MPx, QCISD(T), or CCSD(T)),
2. The method must generate a configuration space small enough that large numbers of electrons (20 for example) are easily handled (satisfied by GVB-PP but not by CASSCF), and
3. The method must be free of any requirement for the user to specify a particular dominant configuration (either MO or VB). Thus the user should need only to specify the number of active electrons and the number of active orbitals (satisfied by CASSCF but not GVB).

Although we refer to the SCF orbital determination followed by the MRCI as the GMO2 method, the SCF method has been previously described as the pair-excited multiconfiguration self-consistent field (PEMCSCF) [14a] and the even replacement multiconfiguration self-consistent field method (ERMC).[14b] In these methods, one specifies the active space as one would for the CASSCF calculation, but one only considers paired excitations between all the orbitals. Thus, for a closed shell molecule, the method is equivalent to a CASSCF with all the configurations having at least one singly occupied orbital eliminated. It is also equivalent to a GVB calculation where one includes all excitations of bonding pairs to other pairs' antibonding orbitals, thus relaxing, in part, the strong orthogonality constraint of the GVB-PP wave function. The PEMCSCF method is different from the earlier proposal by Clementi and Veillard, which only includes paired excitations from a single reference rather than all paired excitations.[15a]

The orbital determination by this method is then followed by a MRCI calculation to relax the restricted spin pairing inherent in the PEMCSCF method. In this paper, we describe a new implementation of this procedure and several applications in which simpler competing methods such as GVB-PP are inadequate. Firstly, we will describe the PEMCSCF wave function and energy; secondly, we will describe the optimization procedure; thirdly, we will describe several examples.

Theoretical Development

The Pair-Excited Multiconfiguration Self-Consistent Field (PEMCSCF) Wave Function. Let n' be the number of CI inactive doubly occupied orbitals φ', n the number of CI active orbitals φ, N the number of CI active electron pairs, and S the

[†] Present address: Université de Marne-la Vallée, M2, Bois de l'Etang, rue Galilee, 77420 Champs sur Marne, France.

[⊗] Abstract published in *Advance ACS Abstracts,* August 15, 1997.

S1089-5639(96)03953-9 CCC: $14.00

TABLE 1: Number of Configuration State Functions (CSF) in the PEMCSCF and CASSCF Calculations for Equal Electrons and Active Orbitals

no. of electrons = no. of orbitals	CASSCF	PEMCSCF
10	19 404	252
14	2 760 615	3 432
18	449 141 836	48 620
22		705 432
24		2 704 156

total spin. The PEMCSCF wave function Ψ can be written as a linear combination of n_{CI} Slater determinants Ψ_i. The determinants are generated by the repartitions (σ) of N electron pairs into ($n - 2S$) orbitals with the same $2S$ orbitals kept singly occupied in all the determinants. All the orbitals are orthogonal, and the total number of electrons is equal to $2(n' + N + S)$.

$$\Psi = \sum_{i=1}^{n_{CI}} C_i \Psi_i$$

$$\Psi_i = |\varphi'_1\bar{\varphi}'_1 \ldots \varphi'_{n'}\bar{\varphi}'_{n'}\varphi_1 \ldots \varphi_{2S}\varphi_{2S+\sigma(i,1)}\bar{\varphi}_{2S+\sigma(i,1)} \cdots \varphi_{2S+\sigma(i,n-2S)}\bar{\varphi}_{2S+\sigma(i,n-2S)}|$$

$$n_{CI} = \binom{n-2S}{N}$$

We report in Table 1 the size of the CI matrix for a case in which the number of active electrons and orbitals is equal and the spin equals zero and compare it with the CI size of an equivalent CASSCF calculation. For a system without any molecular symmetry that would reduce the CI size, the CASSCF method is limited for practical reasons to the optimization of 12−14 active orbitals. The CASSCF configuration interaction size with 14 active orbitals is reached in a PEMCSCF that would optimize 24 active orbitals.

The PEMCSCF wave function is variationally optimized by minimizing the PEMCSCF energy E according to the two sets of variables, the configuration interaction coefficients $\{C_i\}_{i=1,n_{CI}}$ and the orbitals set $\{\varphi_i\}_{i=1,n}$ and $\{\varphi'_j\}_{j=1,n'}$.

$$E = \frac{\langle\Psi|H|\Psi\rangle}{\langle\Psi|\Psi\rangle}$$

$$\left(\frac{\partial E}{\partial \varphi_i}\right) = 0$$

$$\left(\frac{\partial E}{\partial C_j}\right) = 0$$

where i varies from 1 to $n + n'$ and j from 1 to n_{CI}. The PEMCSCF energy can be written as

$$E = \frac{\sum_{i,j=1}^{n_{CI}} C_i C_j H_{ij}}{\sum_{i=1}^{n_{CI}} C_i^2} \qquad (1)$$

where H_{ij} is the configuration interaction matrix element:

$$H_{ij} = \langle\Psi_i|H|\Psi_j\rangle$$

Because two different Slater determinants in the configuration interaction differ by two spin orbitals or by more than two, the off-diagonal nonzero matrix elements are equal to an exchange integral K_{kl} (the two Slater determinants differ by one doubly occupied orbital, φ_k in one determinant and φ_l in the interacting determinant)

$$K_{kl} = \int_1\int_2 \varphi_k(1)\,\varphi_l(1)\,\frac{1}{r_{12}}\,\varphi_k(2)\,\varphi_l(2)\,d\tau_1 d\tau_2$$

The diagonal elements of the CI matrix involve only exchange (K_{kl}), Coulomb (J_{kl}), and one-electron (h_k) integrals over the ($n + n'$) orbitals.

$$J_{kl} = \int_1\int_2 \varphi_k(1)\,\varphi_k(1)\,\frac{1}{r_{12}}\,\varphi_l(2)\,\varphi_l(2)\,d\tau_1 d\tau_2$$

$$h_k = \int_1 \varphi_k(1)\left(T - \sum_\alpha \frac{Z_\alpha}{r_{\alpha 1}}\right)\varphi_k(1)\,d\tau_1$$

Thus, the PEMCSCF energy, in terms of one- and two-electron density matrices, can be simplified by introducing a two-dimensional matrix $\boldsymbol{\rho}$ such that

$$E = \sum_{i=1}^{n+n'} \rho_{ii}(2h_i + J_{ii}) + \sum_{i<j}^{n+n'} \rho_{ij}J_{ij} + \sum_{i>j}^{n+n'} \rho_{ij}K_{ij} + \sum_{\alpha>\beta} \frac{Z_\alpha Z_\beta}{R_{\alpha\beta}} \qquad (2)$$

The one-electron density matrix in the PEMCSCF formulation is a diagonal matrix whose elements are the diagonal elements of the matrix $\boldsymbol{\rho}$. Thus, the PEMCSCF orbitals are the natural orbitals and ρ_{ii} is the occupation number of the orbital φ_i. In the usual notation, $\rho_{ij} = \Gamma_{iijj}$ for $i < j$ and $\rho_{ij} = \Gamma_{ijij}$ for $i > j$.

Mathematical Development of the Wave Function Optimization Procedure. The first step in the optimization procedure is to calculate the matrix $\boldsymbol{\rho}$ referred to as the pseudo-density matrix in the rest of the article. This calculation involves performing the configuration interaction to obtain the coefficients $\{C_i\}_{i=1,n_{CI}}$. The CI algorithm can take full advantage of the fact that the list of integrals needed to perform the configuration interaction calculation can fit in one small two-dimensional matrix. The active orbitals are separated in two sets (of size as equal as possible n1 and n2). A Slater determinant is then encoded by two addresses a1 and a2

$$\mathrm{a1} = \sum_{i=1}^{\mathrm{n1}} \mathrm{occ}_{\mathrm{set1}}(i)2^{i-1}$$

$$\mathrm{a2} = \sum_{i=1}^{\mathrm{n2}} \mathrm{occ}_{\mathrm{set2}}(i)2^{i-1}$$

where $\mathrm{occ}_{\mathrm{set1}}$ and $\mathrm{occ}_{\mathrm{set2}}$ are the active orbital's occupation of the electronic configuration in set1 and set2, respectively. The variable occ is equal to 1 if the orbital is doubly occupied, 0 otherwise. The number of the Slater determinant in the list of determinants is then stored in a two-dimension matrix **A** at the address (a1, a2). The dimension of **A** is equal to $2^{\max(n1,n2)}$ and reaches 2048 for a case in which 22 orbitals are to be optimized. The size of this array corresponds to 17 MB of computer memory, and thus it can be handled on a workstation with 32 MB of memory and 500 MB of disk space.

After all the Slater determinants have been encoded into a single implicit FORTRAN loop, the same configuration generation is then repeated to calculate the nonzero CI matrix elements by generating the doubly excited configurations of the current one: the CI matrix element is equal to K_{ij} where φ_i is the annihilated doubly occupied orbital and φ_j the created one. The previously defined a1 and a2 are calculated for the interacting configuration and A(a1,a2) gives the absolute address of this configuration in the list. The calculation of the lowest eigenvectors and the associated energies is obtained by using a

conjugate gradient algorithm. Calculations with 20 CI active orbitals (CI size = 184 756) have been performed on a Silicon Graphics Inc. Indigo R4400 and take 110 CPU seconds for generating the complete CI matrix. The pseudo-density matrix can be calculated by repeating the CI algorithm, and when the CI matrix element between configurations a and b equals K_{kl} (a different from b), the contribution C_aC_b is added to ρ_{kl} ($k > l$). The elements ρ_{kl} ($k < l$) are calculated by adding the contribution C_a^2 when the Coulomb integral J_{kl} is involved in the calculation of the diagonal CI element of configuration a.

In order to reduce the number of iterations and efficiently control the convergence of the optimization process, a quadratically convergent algorithm is preferred to a Fock matrix type algorithm. This technique also has the advantage of allowing the user to freeze orbitals (CI active or inactive) and is useful in resolving problematic or undesirable rotations between orbitals.

Using Lévy's proposal,[16] the orbitals at iteration (iter+1) are expanded in the basis of the orbitals at iteration (iter) by a unitary transformation in the form of the exponential of a skew-symmetric matrix **X**.

$$\varphi_i^{(\text{iter}+1)}(X) = \sum_j \exp(X)_{ij}\varphi_j^{(\text{iter})} \tag{3}$$

$${}^t\mathbf{X} = -\mathbf{X}$$

The variational equations can be written in terms of the orbital rotation variables X_{ij} and the CI coefficients C_k.

$$\left(\frac{\partial E}{\partial X_{ij}}\right) = 0$$

$$\left(\frac{\partial E}{\partial C_k}\right) = 0 \tag{4}$$

where X_{ij} is an active rotation and k varies from 1 to n_{CI}.

Two algorithms are then possible:

1. The two-step Newton−Raphson consecutively solves the two equations. The second equation (i.e., performing the CI calculation) is solved every iteration. The pseudo-density matrix is then calculated, the energy is expanded in a Taylor series in the variables X_{ij}, and the first equation is solved by a Newton−Raphson procedure.

2. The one-step Newton−Raphson simultaneously solves the two equations. The second equation is solved at the first iteration and then the energy is expanded in a Taylor series in the variables X_{ij} and C_k. Equations 4 are then solved by a Newton−Raphson algorithm.[17]

Although the two-step Newton−Raphson algorithm is not quadratically convergent, it can be used even for very large calculations. The one-step Newton−Raphson has the advantage of quadratic convergence, but the Hessian size (coupling between rotations and CI variables in particular) limits the method to less than 100 000 Slater determinants (at most 18 active CI orbitals and 18 active electrons) on a standard workstation.

The Newton−Raphson Equations. The total energy at iteration (iter+1) is expanded in a Taylor series in the variables $\{x_i\}_{i=1,n_{\text{var}}}$ x is represented as a linear vector of the variables X_{ij} and C_k, n_{var} being the total number of variables

$$E^{(\text{iter}+1)}(x) = E^{(\text{iter})}(x{=}0) + \sum_{i=1}^{n_{\text{var}}} g_i(x{=}0)\cdot x_i + \frac{1}{2}\sum_{i,j=1}^{n_{\text{var}}} x_i\cdot \text{Hess}_{ij}(x{=}0)\cdot x_j \tag{5}$$

where the gradient and the Hessian matrix elements can be derived using eqs 1 and 2

$$g_k(x{=}0) = \left(\frac{\partial E}{\partial x_k}\right)_{x=0} = \sum_{i=1}^{n+n'}\rho_{ii}\left(2\frac{\partial h_i}{\partial x_k} + \frac{\partial J_{ii}}{\partial x_k}\right) + \sum_{i<j}^{n+n'}\rho_{ij}\frac{\partial J_{ij}}{\partial x_k} + \sum_{i>j}^{n+n'}\rho_{ij}\frac{\partial K_{ij}}{\partial x_k} \tag{5a}$$

Even in the one-step Newton−Raphson algorithm the configuration interaction is realized efficiently every iteration, and thus eq 5, which gives a 0 if the variable x_k is a CI coefficient, is exact. The Hessian matrix can be decomposed into three blocks:

The orbital Hessian, second derivative of the energy with respect to two orbital rotation parameters:

$$\left(\frac{\partial^2 E}{\partial X_{\text{ab}}\partial X_{\text{cd}}}\right)_{x=0} = \sum_{i=1}^{n+n'}\rho_{ii}\left(2\frac{\partial^2 h_i}{\partial X_{\text{ab}}\partial X_{\text{cd}}} + \frac{\partial^2 J_{ii}}{\partial X_{\text{ab}}\partial X_{\text{cd}}}\right) + \sum_{i<j}^{n+n'}\rho_{ij}\frac{\partial^2 J_{ij}}{\partial X_{\text{ab}}\partial X_{\text{cd}}} + \sum_{i>j}^{n+n'}\rho_{ij}\frac{\partial^2 K_{ij}}{\partial X_{\text{ab}}\partial X_{\text{cd}}} \tag{5b}$$

The CI Hessian, second derivative of the energy with respect to two CI coefficients:

$$\frac{1}{2}\left(\frac{\partial^2 E}{\partial C_{\text{a}}\partial C_{\text{b}}}\right)_{x=0} = H_{ab} - \delta_{\text{a}}^{\text{b}}E \tag{5c}$$

where $\delta_{\text{a}}^{\text{b}}$ equals 1 if a equals b and 0 otherwise.

The mixed Hessian, second derivative of the energy with respect to one CI coefficient and one orbital rotation variable:

$$\frac{1}{2}\left(\frac{\partial^2 E}{\partial C_{\text{a}}\partial X_{\text{bc}}}\right)_{x=0} = \sum_{i=1}^{n_{\text{CI}}} C_i\frac{\partial H_{\text{a}i}}{\partial X_{\text{bc}}} - C_{\text{a}}\cdot\left(\frac{\partial E}{\partial X_{\text{bc}}}\right)_{x=0} \tag{5d}$$

Applying the variational theorem to the second-order energy development

$$\left(\frac{\partial E}{\partial X_k}\right) = 0 \tag{6}$$

gives the Newton−Raphson set of linear equations: $\forall i = 1, n_{\text{var}}$

$$\sum_{j=1}^{n_{\text{var}}}\text{Hess}_{ij}(x{=}0)x_j = -g_i(x{=}0) \tag{7}$$

Since the following equation is always satisfied

$$\sum_{\text{a}=1}^{n_{\text{CI}}}\left(\frac{\partial^2 E}{\partial C_{\text{a}}\partial X_{\text{bc}}}\right)_{x=0} C_{\text{a}} = 0$$

the Hessian matrix has a zero eigenvalue for the vector that corresponds to the CI eigenvector associated with the eigenvalue E. Different techniques can be used to remedy the problem, and Bisson's shift technique[18] has been implemented. A projector P_{CI} is added to the CI Hessian matrix that removes the intrinsic eigenvalue without perturbing the convergence.

$$P_{\text{CI}} = |\Psi\rangle\ e_0\ \langle\Psi|$$

where e_0 is a large positive number.

The Newton−Raphson eq 7 can be solved by a Choleski decomposition technique[17] for cases of moderate Hessian size

(3000−5000). For larger cases, the preconditioned generalized minimum residual[17] (GMRES) method is more appropriate.

In the cases where the Hessian matrix has negative eigenvalues, a modified constraint algorithm of Fletcher[19] has been implemented. A submatrix of small size (100−300) is extracted from the Hessian matrix, corresponding to its smallest diagonal elements and the largest elements of the gradient vector. The exact constraint algorithm of Fletcher is then applied to this submatrix, and since it is small, a Givens diagonalization can be performed at a low cost. The optimized shift can then be used in the GMRES algorithm.[20] The inverse of the submatrix is easily calculated after diagonalization and supplies us a preconditioning matrix of choice for the GMRES method. The solution of eq 7 leads to an updated set of molecular orbitals that are used in an iterative process until both the gradient and the step in the rotation variable space are simultaneously lower than a small threshold (typically 10^{-6}).

The Rotation Variables. Contrary to CASSCF calculations, the energy is not invariant upon rotations among the CI active occupied orbitals.[21] These rotations have to be included in the variable set as well as the rotations between doubly occupied and CI active orbitals. Rotations among doubly occupied orbitals and rotations among singly occupied are redundant and thus are removed from the orbital optimization set.

A second-order Taylor series for eq 3 can be written for all the occupied orbitals:

$$\varphi_i^{(\kappa+1)}(X) = \varphi_i^{(\kappa)} + \sum_{j=1}^{n_{\text{basis}}} X_{ij}\varphi_i^{(\kappa)} + \sum_{j=1}^{n_{\text{basis}}}\sum_{k=1}^{n_{\text{basis}}} X_{ik}X_{kj}\varphi_i^{(\kappa)}$$

It appears from the second-order expansion that $\varphi_i^{(\kappa+1)}$ is a function of rotations among virtual orbitals. However, for o and o′ occupied orbitals and v, v′,v″, and v‴ virtual orbitals, the following equation is verified

$$\left(\frac{\partial^2 E}{\partial X_{\text{oo}'}\partial X_{\text{vv}'}}\right)_{X=0} = \left(\frac{\partial^2 E}{\partial X_{\text{vv}'}\partial X_{\text{v}''\text{v}'''}}\right)_{X=0} = 0$$

while eq 8 is only satisfied at convergence:

$$\left(\frac{\partial^2 E}{\partial X_{\text{vo}}\partial X_{\text{v}'\text{v}''}}\right)_{X=0} = 0 \qquad (8)$$

The convergence properties are not altered assuming that this matrix element is always equal to zero.[22] Rotations among virtual orbitals are thus removed from the variable set. The matrix of the rotations **X** (orbital variables of the problem) has the following structure.

occupied orbitals	virtual orbitals
A	**B**
^{t}**B**	0

where $^t\mathbf{A} = -\mathbf{A}$, **A** is the submatrix of the rotation among occupied orbitals, and **B** is the submatrix of the rotation coupling occupied and virtual orbitals.

TABLE 2: Study of CH_4. Total Energy and Number of Iterations To Converge the PEMCSCF Calculation by Optimizing Rotations among Occupied Orbitals

strongly occupied orbitals	weakly occupied orbitals	total PEMCSCF energy (au)	no. of iterations
symmetry-adapted	symmetry-adapted	−40.243 417	4
symmetry-adapted	bond-type orbitals	−40.261 522	16
bond-type orbitals	symmetry-adapted	−40.261 522	16
bond-type orbitals	bond-type orbitals	−40.261 522	3

The second-order Taylor series can then be written as: $\forall i = 1, n + n'$

$$\varphi_i^{(\kappa+1)}(X) = \varphi_i^{(\kappa)} + \sum_{j=1}^{n_{\text{basis}}} X_{ij}\varphi_i^{(\kappa)} + \sum_{j=1}^{n_{\text{basis}}n_{\text{occupied}}}\sum_{k=1} X_{ik}X_{kj}\varphi_i^{(\kappa)} \qquad (9)$$

The Preoptimization Process: Orbital Localization. Several authors[10] have pointed out that rotations among occupied orbitals are somewhat problematic. A first step in the calculation only optimizes the rotation among the occupied orbitals using the guess orbital space. Since the number of occupied orbitals that have to be optimized is relatively small, the four-index transformation of the two-electron integrals, performed every MCSCF iteration, can be done in memory at a low cost. The transformation from the atomic basis set to the molecular basis set is performed once at the first iteration. This process defines an intrinsic *localization method*; several properties of the preoptimization algorithm may be illustrated on an example.

Study of CH_4. A quadruple-ζ[23] + polarization basis set [C(13s7p1d/8s4p1d), H(9s1p,4s1p) α_d(C) = 0.75 and α_p(H) = 1.15] was used for this case at a tetrahedral geometry of CH_4. The CH distance was fixed at 2.052 282 a_0. The total Hartree−Fock energy in this basis set is −40.214 360 au. The guess orbital space is constructed with the five occupied HF orbitals (one doubly occupied and four strongly occupied orbitals) and four antibonding orbitals obtained by external projection of the 1s atomic orbitals of the H atom (weakly occupied orbitals) in the PEMCSCF calculation. All these orbitals can be combined to form symmetry-adapted orbitals or localized (bond-type) orbitals. This guess orbital space would be a good candidate for a valence CASSCF calculation of CH_4.[24] The 1s orbital of the carbon is doubly occupied in all the Slater determinants but optimized. The initial calculation only optimizes the rotations among the occupied orbitals (no virtual orbitals are involved). Although the two-electron integrals over the basis functions are calculated using symmetry, a two-electron integral four-index transformation has been implemented to calculate the two-electron integrals over MOs that are not symmetry-adapted. However, the symmetry can be constrained by deactivating all the rotations that break the symmetry. The total energy and the number of iterations necessary to get to the convergence are reported in Table 2. While calculations using symmetry-adapted orbitals or localized (bond-type) orbitals converge without difficulty, the Hessian matrix in the former calculations has negative eigenvalues reflecting the fact that a point of lower energy exists. In this particular example, the use of localized (bond-type) orbitals allows convergence to a lower energy. The fast in-core two-electron transformation allows the user to improve the localized (bond-type) guess orbitals for the subsequent step of orbital optimization and thus is referred to as a preoptimization process. Lévy[25] has shown on some examples that the complete multiconfiguration self consistent field theory[26] (CMC), in which a subspace of the PEMCSCF configuration interaction space is used, converges to lower energies using localized (bond-type) orbitals than do symmetry-adapted orbitals. The PEMCSCF results on CH_4 show a similar behavior.

TABLE 3: Study of CH_4. Total Energy, Shift of the Hessian Matrix, Norm of the Gradient Vector, and Norm of the Step X in the Orbital Rotation Space[a]

iteration	energy (au)	shift	|grad|	|x|
1	−40.261 522	0.033 020	0.093 254	0.548 008
2	−40.274 910	0.0	0.020 811	0.235 881
3	−40.275 861	0.0	0.003 051	0.005 855
4	−40.275 863	0.0	0.000 003	0.000 018
5	−40.275 863	0.0	0.000 000	0.000 000

[a] Trust region radius has an initial value of 0.5.

The Optimization Process. The rotations among the occupied orbitals are kept active during the optimization process in which virtual orbitals are added to the occupied in order to be optimized. The values of the Hessian matrix and gradient vector elements are calculated analytically using eqs 5 a−c with the orbital derivative expressions:

$$\left(\frac{\partial \varphi_i}{\partial X_{ab}}\right)_{X=0} = \delta_i^a \varphi_b - \delta_i^b \varphi_a$$

$$\left(\frac{\partial^2 \varphi_i}{\partial X_{ab}\partial X_{cd}}\right)_{X=0} = -\frac{1}{2}[\varphi_d(\delta_i^b\delta_a^c - \delta_i^a\delta_b^c) + \varphi_c(\delta_i^a\delta_b^d - \delta_i^b\delta_a^d) + \varphi_b(\delta_i^d\delta_a^c - \delta_i^c\delta_a^d) + \varphi_a(\delta_i^c\delta_b^d - \delta_i^d\delta_b^c)]$$

The calculation of the Hessian matrix requires integrals that involve at most two virtual orbitals. The orbital Hessian and gradient are calculated by a double Fortran loop over the occupied molecular orbitals where the first and second derivatives of the one-electron, Coulomb, and exchange integrals are calculated analytically. The nontrivial part of the mixed Hessian is calculated directly by reproducing the CI algorithm, and the analytical derivatives of the K_{ij} integrals are calculated as needed and thus do not require any additional memory.

Study of CH_4. Using the preoptimized localized (bond-type) orbitals as guess vectors, the PEMCSCF calculation is performed with an orthogonal complement of the basis set as virtual orbitals. The total energy, norm of the gradient vector, norm of the step **X** and shift of the Hessian matrix are reported in Table 3. The calculation converges in five iterations using the one-step Newton−Raphson algorithm with a threshold on the norm of the gradient equal to 10^{-6}.

The GMO2(SDTQ) Energy Evaluation. Although the PEMCSCF method gives a large amount of correlation energy, it retains some intrinsic problems connected to the absence of configurations with unpaired electrons like dissociation into multiplets and spectroscopic states. However, to fairly compare GMO2 with the CASSCF method, a full CI in the PEMCSCF optimized orbital set should be used, GMO(FCI). While it is possible to optimize 18 orbitals with 18 active CI electrons using the PEMCSCF method, the full CI calculation in the space of these 18 orbitals is beyond reach.[27] In the mean time, it is likely that there is only a small number of CSF in this full-CI calculation that have an important effect. Thus, an alternative, invoking only single, double, triple, and quadruple excitations (GMO2(SDTQ)), has been developed for large applications.

For the GMO2(SDTQ) calculations, a full CI calculation is performed only within the strongly occupied orbitals of the PEMCSCF (orbitals with a PEMCSCF occupation number greater than some tolerance, say 0.4) and subsequently followed by all the single, double, triple, and quadruple excitations (SDTQ) of all the possible active orbitals from this CAS reference space into the rest of the optimized orbitals. As the CI size increases drastically with the number of orbitals and active electrons, the triple and quadruple excitations can be restricted to a small dimension orbital subspace (orbitals with a PEMCSCF occupation number greater than some tolerance, say 0.1), while performing all the single and double excitations from the references to the remainder of the complete optimized orbital space. The total energy will be higher than the CAS CI total energy, GMO(FCI), but should take into account a large fraction of the CAS correlation energy and include important effects of spin recoupling.

SCHEME 1

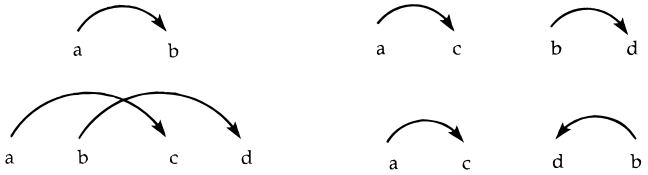

To take into account dynamical correlation effects, the GMO2(SDTQ) procedure can be used to isolate a configuration reference space for subsequent MRCI calculations with excitations outside the optimized orbital space.

The GMO2(SDTQ) configuration interaction program is developed to minimize the amount of memory and disk space needed. The two-electron integral list over the PEMCSCF optimized orbitals is, in all the cases, small enough to be stored in memory at all time, roughly proportional to $n^4/8$. The process implicitly builds the list of configurations and for each electronic configuration generates only the singly and doubly excited configurations interacting *a priori* with the current one, by using the following pattern (see Scheme 1). Double excitations are possible from orbital φ_a and φ_b, doubly or singly occupied in the current configuration to orbital φ_c and φ_d, singly occupied or unoccupied in the current configuration. The single excitation is realized from orbital φ_a to orbital φ_b.[28]

This pattern generates all the possible interacting doublets of configurations without repetition. When two interacting electronic configurations (I and J) are generated, the list of Slater determinants of configuration I is implicitly constructed, and only the nonzero CI matrix elements are evaluated by generating the Slater determinants of configuration J that are singly and doubly excited from the current determinant. The value of the CI matrix element is easily obtained and most of the effort is devoted to calculating the *address* of the generated determinant in the list of the determinants of configuration J. This address is a function of the number of unpaired electrons in configuration J. By restricting the excitation in GMO2(SDTQ) to quadruple excitations, the arbitrary limit of 14 unpaired electrons does not represent a restriction but allows us to encode a determinant by using a technique similar to that in section 3.[29]

$$\text{address} = \sum_{i=1}^{n_{\text{unpaired electrons}}} \text{occ}(i)2^{i-1}$$

where occ equals 0 for an α spin and 1 for a β spin.

The block of CI matrix expressed in the basis of Slater determinants can be transformed easily to a spin-adapted configuration state function basis if necessary. The program calculates the lowest eigenvalues of this CI matrix with a conjugate gradient algorithm recalculating the CI matrix every iteration.

Study of CH_4. To evaluate the quality of the GMO2 method, the GMO2(FCI) and GMO2(SDTQ) energies are compared to the CASSCF energy. In Table 4, the total energies are reported for CH_4 using the symmetry-adapted optimized PEMCSCF orbitals or the localized (bond-type) orbitals. The CASSCF energy is lower than the GMO2(FCI) by 2.8 kcal/mol when the PEMCSCF is constrained to converge to symmetry-adapted orbitals and by 3.0 kcal/mol when the localized orbital solution

TABLE 4: Total Energy of CH_4 at Different Levels of Theory: Hartree−Fock, PEMCSCF, GMO2(SDTQ), GMO2(FCI), and CASSCF[a]

method	total energy (au) localized (bond-type) orbitals	total energy (au) symmetry-adapted orbitals
HF	−40.214 360	
PEMCSCF	−40.275 863 (13.2)	−40.247 861 (30.2)
GMO2(SDTQ)	−40.292 123 (3.1)	−40.292 463 (2.8)
GMO2(FCI)	−40.292 161 (3.0)	−40.292 521 (2.8)
CASSCF	−40.296 988	

[a] Energy differences from the CASSCF energy in kcal/mol.

TABLE 5: Total Energy of H_4 at the GVB-PP, GVB-PP(FCI), PEMCSCF, GMO2(FCI), and CASSCF Levels of Theory[a]

	localized (bond-type) orbitals (au)	symmetry-adapted orbitals (au)
GVB-PP	−2.037 91	−1.984 90
GVB-PP(FCI)	−2.060 37 (9.9)	−2.049 89 (16.5)
PEMCSCF	−2.037 91	−2.002 57
GMO2(FCI)	−2.060 37 (9.9)	−2.069 64 (4.1)
CASSCF	−2.076 17	

[a] Energy differences from the CASSCF energy in kcal/mol.

TABLE 6: Total Energy of Benzene at Different Levels of Theory: Hartree−Fock, PEMCSCF, GMO2(FCI), and CASSCF with Localized (Bond-Type) Orbitals and Symmetry-Adapted Orbitals[a]

	localized (bond-type) orbitals (au)	symmetry-adapted orbitals (au)
HF	−230.673 65	
PEMCSCF	−230.718 27	−230.704 35
GMO2(FCI)	−230.744 63 (2.3)	−230.747 48 (0.5)
CASSCF	−230.748 25	

[a] Energy differences from the CASSCF energy in kcal/mol.

is used. These small differences can be interpreted as the effect of configurations with unpaired electrons on the orbital optimization. These differences represent only 5.8% of the correlation energy at the CASSCF level. GMO2(SDTQ) is only higher than the GMO2(FCI) by a fraction of a kcal/mol and thus represents an accurate approximation of GMO2(FCI).

The GMO2 localization procedure is illustrated in the study of a square H_4 system and in the study of the ground state of benzene. In order to calculate relative energies and test the reliability of the GMO2 procedure, the linear dissociation of multiple bonds is studied with two examples: N_2 and C_2H_2.

Results and Discussion

Study of the GMO2 Localization Procedure in a Square H_4 System. In the planar H exchange reaction of H_2 with H_2, the transition state of the system is characterized by a square geometry. While the GVB-PP method can represent the reactants and products of the reaction by a perfect pairing of two electron pairs, this method is unsuitable to calculate the energy of the square transition state. GVB-PP(FCI), GMO2-(FCI) and CASSCF calculations were performed using a quadruple-ζ[23] + polarization basis set H (9s1p/4s1p) (α_p(H) = 1.0) at the CASSCF optimized geometry (d_{HH} = 1.287 76 au) of the transition state. PEMCSCF and GVB-PP calculations are performed using both delocalized D_{4h} symmetry orbitals and localized orbitals. The results are presented in Table 5. The GVB-PP and PEMCSCF procedures converge to a similar energy (if not equal) using localized orbitals in both calculations. These localized orbitals are described by two H−H bonds and two H−H antibonds. Performing the FCI in these optimized orbitals gives an energy difference equal to 9.9 kcal/mol compared to the CASSCF energy. Using symmetry-adapted (delocalized) orbitals, the GVB-PP converges to a higher energy and the FCI performed with the optimized orbitals is 16.5 kcal/mol higher than the CASSCF energy. While the PEMCSCF procedure converges to higher energy when constraining the orbitals to be symmetry-adapted, the GMO2(FCI) energy is only 4.1 kcal/mol higher than the CASSCF energy.

GMO2 Study of the Localization Process in Benzene. The geometry of the benzene molecule was optimized at the Hartree−Fock level using a triple-ζ basis set[30] for C(10s6p/5s3p) and H(5s/3s). The CC and CH bond distances are equal to 1.387 and 1.073 Å, respectively. GMO2 and CASSCF calculations were performed at this geometry in the π orbitals of the molecule only (six electrons in six orbitals). The Hartree−Fock σ_{CH} and σ_{CC} were kept frozen in the calculations, and we focus here on the localization of the orbitals within the π system of benzene and its effect on the energy. For the GMO2 calculation, guess orbitals are constructed using the three HF occupied orbitals and three virtual orbitals obtained by external projection of ad-hoc carbon 2p orbital combinations. These orbitals are D_{6h} symmetry-adapted (delocalized) orbitals. The first step in the GMO2 calculation is to preoptimize the guess vectors. At the first iteration, the Hessian matrix has three negative eigenvalues whose respective eigenvectors are orthogonal to the gradient vector. These eigenvectors represent the simultaneous mixing of the strongly occupied orbitals among themselves and of the weakly occupied among themselves. Although the Newton−Raphson algorithm optimizes an orbital step orthogonal to these eigenvectors, the final orbital step is obtained by adding a linear combination of these eigenvectors to the Newton−Raphson step. At the second iteration, the Hessian matrix has negative eigenvalues nonorthogonal to the gradient vector, and thus the orbital step is optimized using the constrained algorithm of Fletcher. The preoptimization process converges then to localized orbitals. These orbitals are finally fully optimized by completing the π basis set with virtual π orbitals. At the PEMCSCF level of theory, the electronic structure can be interpreted as a Kekulé structure where the pair excitation from a bond orbital to its corresponding antibonding localized orbital maximizes the electron correlation. The GMO2 calculation is completed by performing a full CI calculation in the π orbitals. The GMO2(FCI) energy is higher than the π-CASSCF energy by only 2.3 kcal/mol.

The optimized GMO2 localized orbitals can be transformed to symmetry-adapted orbitals by appropriate linear combination. A second GMO2 calculation was performed constraining the orbitals to be symmetry-adapted. Although the PEMCSCF energy is then 8.7 kcal/mol higher in energy than the PEMCSCF energy calculated with localized orbitals, the GMO2(FCI) energy using the symmetry-adapted orbitals is only 0.7 kcal/mol higher than the CASSCF energy of benzene.

Although the PEMCSCF procedure tends to converge to lower energies using localized orbitals than symmetry-adapted (delocalized) ones, the GMO2(FCI) energy is lower using symmetry-adapted orbitals and gives results closer in energy to the CASSCF results. The GMO2 energy may result in a lower energy using localized orbitals for larger systems, in which the localized bond−antibond excitations may play a dominant role, especially at the SDTQ level.

GMO2 Study of the Linear Dissociation of Multiple Bonds. In order to investigate the eventual deficiencies of GMO2 compared to CASSCF, multiple bond breaking is studied in two examples. Since GMO2's orbitals are optimized in a

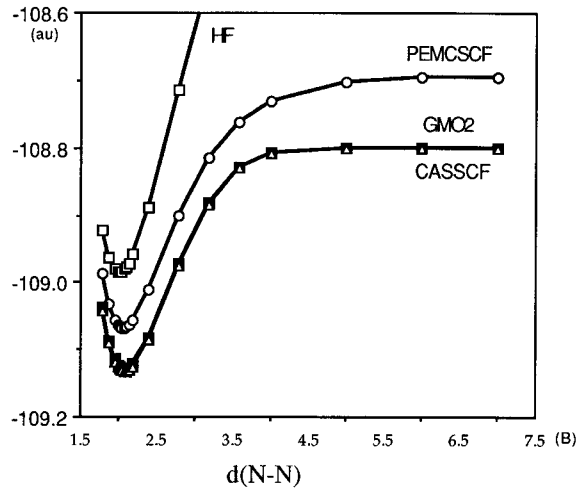

Figure 1. Potential energy of N_2 $^1\Sigma g^+$ at various levels of theory.

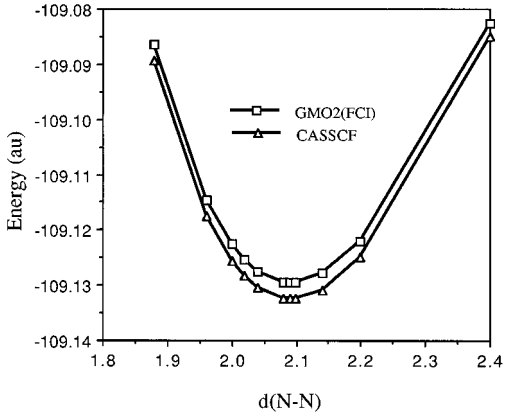

Figure 2. Potential energy of N_2 $^1\Sigma g^+$ near the equilibrium bond distance at GMO2 and CASSCF levels of theory.

calculation involving only pair electron (PE) excitations, it is expected that the dissociation into high-spin fragments may be problematic. However, the spin recoupling in GMO2 is made possible by the configuration interaction using PE-optimized orbitals.

GMO2 Study the Linear Dissociation of N_2. A quadruple-ζ^{23} + polarization N(13s7p1d/8s4p1d) ($\alpha_d = 1.0$) basis set was used in the following calculations. The potential energy surface was calculated at several levels of theory, HF, PEMCSCF, GMO2(FCI) and CASSCF (Figure 1). The active CI orbital space in the optimization of the orbitals in the GMO2 and CASSCF calculations is composed of one nonbonding orbital on each nitrogen atom, three bonding orbitals (σ, π_x, and π_y) and their corresponding antibonding orbitals (σ^*, π_x^*, and π_y^*). In this orbital space, the CASSCF dissociation limit for the ground state $X^1\Sigma_g^+$ is the singlet coupling of two nitrogen atoms in their ground state $^4S-(s^2p^3)$. Although the N_2 triple bond may be represented at the equilibrium distance by a perfect-pairing GVB reference, the asymptotic value of the GVB-PP energy does not represent the singlet coupling of two ^4S nitrogen atoms. The PEMCSCF wave function shows a similar behavior and does not dissociate into two nitrogen ground state atoms. While the correct spin coupling is prohibited by both GVB-PP and PEMCSCF wave functions, using the orbitals optimized by the PEMCSCF procedure in a full configuration interaction reproduces the CASSCF energy accurately. The maximum energy difference between the CASSCF energy and the GMO2-(FCI) energy is obtained for a internuclear distance close to the equilibrium geometry and is less than 2 kcal/mol, see Figure 2. Thus, the GMO2 procedure can reliably predict spin recoupling and multiple-bond breaking.

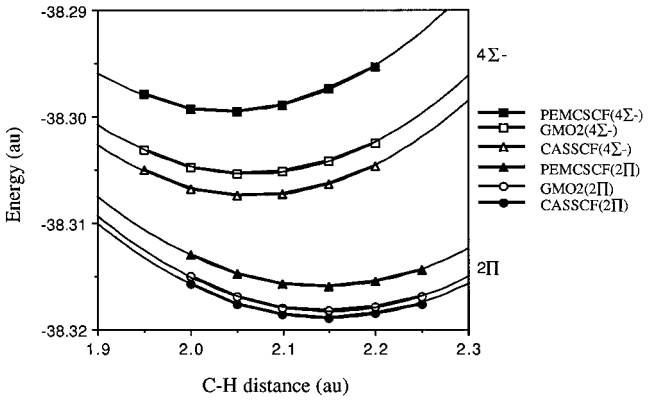

Figure 3. Potential energy curves for $^2\Pi$ and $^4\Sigma^-$ states of CH at various levels of theory.

GMO2 Study of the Linear Dissociation of C_2H_2. While the linear dissociation of C_2H_2 into two CH fragments overlaps with the previous study as it is also a multiple-bond-breaking reaction, the spin-recoupling effects are different because the ground state of CH is a $^2\Pi$ at the CASSCF level instead of a $^4\Sigma^-$, which is the HF ground state of CH. A quadruple-ζ^{23} + polarization basis set: C(13s7p1d/8s4p1d), H (9s1p/4s1p) (α_d-(C) = 0.85 and α_p(H) = 0.95) was used in this study. A CASSCF calculation involving only CC bonds would dissociate C_2H_2 into two fragments CH ($^4\Sigma^-$) with an energy profile similar to the one calculated for N_2. A complete valence CASSCF (10 electrons/10 orbitals) would dissociate into two fragments CH ($^2\Pi$).

GMO2 and CASSCF calculations were performed on the $^4\Sigma^-$ and $^2\Pi$ states of CH and on the $X^1\Sigma_g^+$ ground state of C_2H_2. The GMO2 study of CH $^4\Sigma^-$ was performed by optimizing five orbitals: two singly occupied π_x and π_y orbitals, one singly occupied nonbonding orbital, the bonding σ_{CH} orbital, and a correlating antibonding σ_{CH}^*, the latter two with variable occupancy. The GMO2 study of the $^2\Pi$ state of CH was performed by also optimizing five orbitals: one singly occupied π_x orbital, two strongly occupied σ orbitals, one weakly occupied σ_{CH}^* orbital, and the weakly occupied π_y orbital. For both states, a GMO2(FCI) was performed using the optimized orbital space and compared to a CASSCF calculation in an equivalent space.[31] The results are presented in Figure 3. Both GMO2 and CASSCF energy curves present a minimum for the same CH distances: the equilibrium distance is equal to 2.15 au for the $^2\Pi$ state and 2.05 au for $^4\Sigma^-$. The energy difference between GMO2 and CASSCF is constant for CH distances close to the equilibrium geometry and is equal to 0.4 and 1.2 kcal/mol for the $^2\Pi$ and $^4\Sigma^-$ states, respectively.

The energy profile of the C_2H_2 linear dissociation reaction can be separated into two regions:

1. *CC distance ranging from 2.0 to 3.6 au.* In this region, the HF reference is dominant and can be interpreted as a triple bond. The CH bond distance is optimized at the CASSCF level. The potential energy curve in this region is calculated at several levels of theory, HF, PEMCSCF, GMO2(SDTQ), GMO2(FCI), and CASSCF, and represented in Figure 4. The GMO2(SDTQ) is performed with a reference configuration space restricted to a single Slater determinant built with the strongly occupied orbitals of the PEMCSCF calculation. In this region, the maximum energy difference between GMO2(SDTQ) and GMO2-(FCI) is small (less than 0.3 kcal/mol at the equilibrium geometry) and becomes significant (equal to 2 kcal/mol) when the π^* orbitals' occupancy reaches 0.283 for a CC distance equal to 3.3 au. It is likely that configurations involving an orbital with an occupancy higher than 0.3 must be included in the reference space for the GMO2(SDTQ). The energy difference

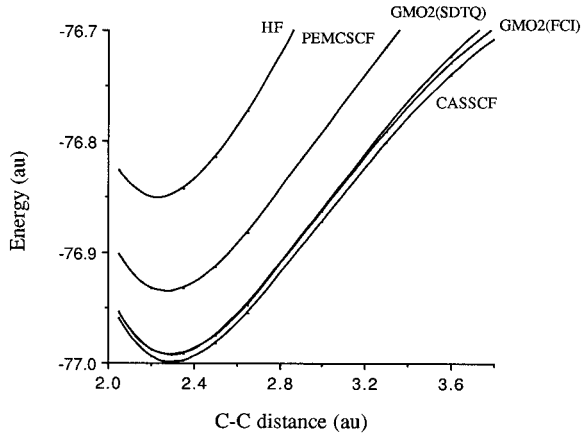

Figure 4. Potential energy curves for the C_2H_2 $^1\Sigma g^+$ state at various levels of theory for bond distances between 2.0 and 3.6 au.

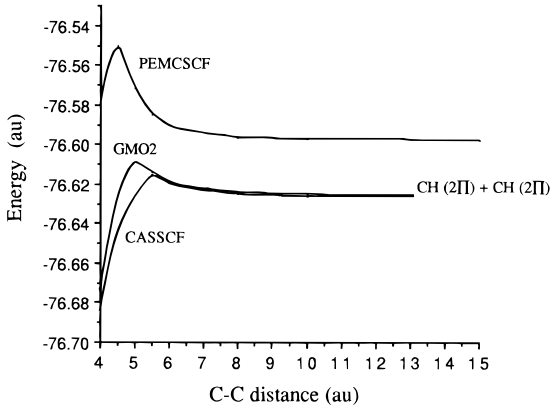

Figure 5. Potential energy curves for the C_2H_2 $^1\Sigma g^+$ state at various levels of theory for bond distances beyond 3.6 au.

between the GMO(FCI) and CASSCF results increases from 3.3 to 6.5 with the CC bond distance. At the equilibrium geometry, the difference is equal to 4.0 kcal/mol (2.4 kcal/mol of this difference is from the isolated fragments CH $^4\Sigma^-$), and is small compared to the value of the electron correlation energy at the CASSCF level (95 kcal/mol). This energy difference is also small compared to the contribution to the total energy of electronic configurations with unpaired electrons, a value equal to the difference between the GMO2(FCI) and PEMCSCF energies (36.5 kcal/mol).

2. *CC distance ranging from 3.6 to 15 au.* For intermediate CC distances, an avoided crossing between an attractive covalent $^1\Sigma_g^+$ arising from the singlet coupling of two CH $^4\Sigma^-$ states and a repulsive $^1\Sigma_g^+$ arising from the singlet coupling of two CH $^2\Pi$ states is predicted. The challenge of GMO2 is then to correctly describe the complete change in the wave function (CI coefficients and orbitals). The potential energy curve is given in Figure 5 at the PEMCSCF, GMO2(FCI) and CASSCF levels. Apart from the avoided crossing that occurs in that region, the repulsive $^1\Delta_g$ state of C_2H_2 is close in energy to the $^1\Sigma_g^+$. However, at the PEMCSCF level, these two states do not mix and the Δ_g state is easily identified by the fact that the CI coefficient on the configuration $\sigma_{CH}^2\sigma_{CH}^2\sigma_{CC}^2\pi_x^2\pi_y^2$ is equal to zero. An excited state optimization procedure has been implemented in the GMO2 code. At the CASSCF level of theory, the nature of the wave function changes for a CC distance close to 5.5 au. The optimized CH bond distance changes from a value that is close to the optimized equilibrium bond distance in CH $^4\Sigma^-$ to a value close to that in CH $^2\Pi$ (see Figure 6). Depending on the guess vectors used to initialize the GMO2 optimization, the calculation for the CC distance equal to 4.5 au converges to two $^1\Sigma_g^+$ wave functions, both first roots of the PEMCSCF configuration interaction with

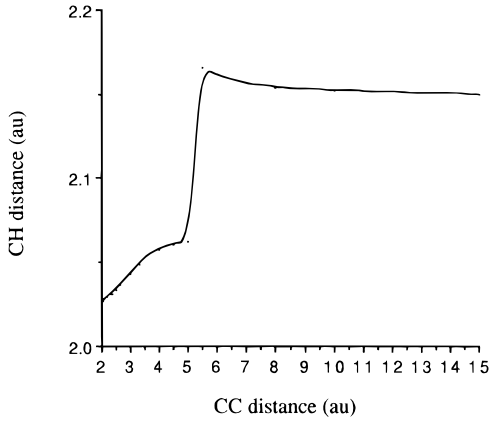

Figure 6. CH bond distances as a function of CC bond distances for dissociation of the $^1\Sigma g^+$ state of C_2H_2 at the CASSCF level.

TABLE 7: Total Energy (au) of C_2H_2 for a CC Internuclear Distance of 4.5 au at the PEMCSCF, GMO2(FCI), and CASSCF Levels of Theory. Two Sets of Orbitals Are Optimized for the First Root of the PEMCSCF Calculation

	orbital set 1	orbital set 2
PEMCSCF	−76.550 44	−76.519 90
GMO2(FCI)	−76.625 53	−76.632 00
CASSCF	−76.643 47	

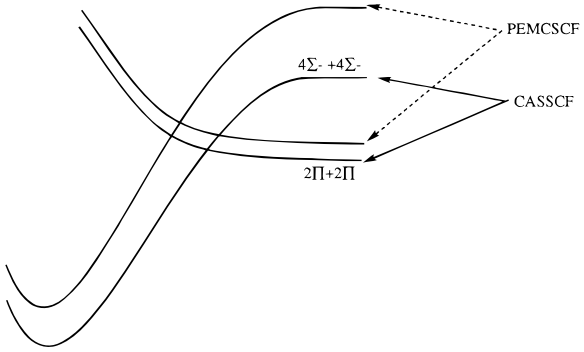

Figure 7. Schematic representation of diabatic energy curves at the CASSCF and PEMCSCF levels.

different associated energies and different CI expansions. A GMO2(FCI) performed with these optimized orbitals gives two different energies. In Table 7, the total energies of the PEMCSCF, GMO2, and CASSCF calculations are reported. The CASSCF results are comparable to the GMO2 (FCI) results obtained with the orbital set 2 since the CI expansions are similar. Thus, the PEMCSCF calculation reflects that the crossing has already occurred. The effect of the spin-coupling constraints at the PEMCSCF level are illustrated by a schematic representation of diabatic energy curves (at the CASSCF and PEMCSCF levels) in Figure 7. The PEMCSCF wave function that dissociates into two CH ($^4\Sigma^-$) is constrained to a perfect-pairing coupling of the two fragments. The difference in energy with the CASSCF dissociation energy is larger than the equivalent difference concerning the dissociation into two CH ($^2\Pi$) fragments. Although the GMO2 procedure depends essentially on the PEMCSCF orbital optimization process, the maximum difference of the total energy is only higher than 7 kcal/mol for CC internuclear distances close to 5.0 au. For long CC distances, the GMO2 and CASSCF energy difference is extremely small (lower than 1 kcal/mol) and close to the difference calculated for the isolated fragments.

Unlike the GVB-PP that would dissociate C_2H_2 into two CH ($^4\Sigma^-$) fragments, the GMO2 procedure takes into account the interaction of low-energy states. The energy difference between GMO2(FCI) and the CASSCF method is small at all geometries.

Conclusion. The GMO2 method, a PEMCSCF orbital optimization followed by a SDTQ configuration interaction energy determination in the active space, is a viable alternative to CASSCF methods when the number of active electrons is very large. In the future, the method may be particularly useful in transition metal systems, where complexes with multiple metal−ligand bonds[32] and dimers with multiple metal−metal bonds or bridging pi−acceptor ligands have significant multireference character. Thus, the technique should be included in our repertoire of restricted active space self-consistent field methods.

Acknowledgment. We thank the Robert A. Welch Foundation (Grant A-648) and the National Science Foundation (Grants CHE91-13634 and 94-23271) for financial support. M.C. thanks B. Lévy, P. Pernot, and P. Archirel (Groupe de Chimie Quantique CNRS, Orsay, France) for valuable discussions and the Ministère des Affaires Étrangères (France) whose authorization allowed this research at Texas A&M University as a CSN.

References and Notes

(1) Roothaan, C. C. J. *Rev. Mod. Phys.* **1951**, *23*, 69.

(2) Møller, C.; Plesset, M. S. *Phys. Rev.* **1934**, *46*, 618. Pople, J. A.; Seeger, R.; Krishnan, R. *Int. J. Quantum Chem. Symp.* **1977**, *11*, 149

(3) Cizek, J. *Adv. Chem. Phys.* **1969**, *14*, 35. Purvis, G. D.; Bartlett, R. J. *J. Chem. Phys.* **1982**, *76*, 1910. Scuseria, G. E.; Janssen, C. L.; Schaefer, H. F., III *J. Chem. Phys.* **1988**, *89*, 7382. Scuseria, G. E.; Schaefer III, H. F. *J. Chem. Phys.* **1989**, *90*, 3700.

(4) Pople, J. A.; Head-Gordon, M.; Raghavachari, K. *J. Chem. Phys.* **1987**, *87*, 5968.

(5) Pople, J. A.; Binkley, J. S.; Seeger, R. *Int. J. Quantum Chem. Symp.* **1976**, *10*, 1.

(6) Shepard, R. In *Advances in Chemical Physics LXIX*; John Wiley & Sons: New York, 1987; p 63. Ruedenberg, K.; Schmidt, M. W.; Gilbert, M. M.; Elbert, S. T. *Chem. Phys.* **1982**, *71*, 41. Werner, H.-J.; Knowles, P. J. *J. Chem. Phys.*, **1985**, *82*, 5053.

(7) Roos, B. O. In *Advances in Chemical Physics LXIX*; John Wiley & Sons: New York, 1987; p 447. Siegbahn, P. E. M.; Almlöf, J.; Heiberg, A.; Roos, B. O. *J. Chem. Phys.* **1981**, *74*, 2384.

(8) Goddard, W. A., III; Dunning, T. H., Jr.; Hunt, W. J.; Hay, P. J. *Acc. Chem. Res.*, **1972**, *6*, 368. Bobrowicz, F. W.; Goddard, W. A., III In *Modern Theoretical Chemistry*; Plenum: New York, 1977; Vol. 3, p 79.

(9) Cooper, D. L.; Geratt, J.; Raimondi, M. In *Advances in Chemical Physics LXIX*; John Wiley & Sons: New York, 1987; p 319.

(10) Werner, H. J. In *Advances in Chemical Physics LXIX*; John Wiley & Sons: New York, 1987; p 1. Olsen, J.; Roos, B. O.; Jørgensen, P.; Jensen, H. J. Aa. *J. Chem. Phys.* **1988**, *89*, 2185. Sherrill, C. D.; Schaefer, H. F., III *J. Phys. Chem.* **1996**, *100*, 6069.

(11) Anderson, K.; Blomberg, M. R.; Fülscher, A. M. P.; Kellö,V.; Lindh, R.; Malmquist, P.-Å.; Noga, J.; Olsen, J.; Roos, B. O.; Sadlej, A. J.; Siegbahn, P. E. M.; Urban, M.; Widmark, P.-O. *MOLCAS Version 2 User's Guide*; University of Lund, April 1992.

(12) Hall, M. B. *Chem. Phys. Lett.* **1979**, *61*, 461. Hall, M. B. *Int. J. Quantum Chem.* **1978**, *14*, 613. Hall, M. B. *Int. J. Quantum Chem. Symp.* **1979**, *13*, 195. Hall, M. B. In *Recent Developments and Applications of Multiconfiguration Hartree-Fock Methods*; Dupuis, M. Ed.; NRCC Proceedings No. 10; Nat. Techn. Info: Springfield, VA, 1981; p 31.

(13) Low, A. A.; Hall, M. B. *Inorg. Chem.* **1993**, *32*, 3880.

(14) (a) Carbo, R.; Hernandez, J. A. *Chem. Phys. Lett.* **1977**, *47*, 85. Carbo, R.; Riera, J. M. *A General SCF Theory*; Springer: Berlin, 1978. Yamaguchi, Y.; Osamura, Y.; Goddard, J. D.; Schaefer, H. F., III *A New Dimension to Quantum Chemistry*; Oxford University Press: New York, 1994. (b) Roothaan, C. C. J.; Detrich, J.; Hopper, D. G. *Int. J. Quantum Chem.* **1979**, *S13*, 93. Roothaan, C. C. J.; Detrich, J. *Phys. Rev. A* **1983**, *27*, 29.

(15) Clementi, E.; Veillard, A. *J . Chem. Phys.* **1966**, *44*, 3050.

(16) Lévy, B. Thesis, CNRS No. AO 5271 Paris 1971. Lévy, B. *Int. J. Quantum Chem.* **1970**, *4*, 297. Lévy, B. *Chem. Phys. Lett.* **1973**, *18*, 59.

(17) Press, W. H.; Teukolsky, S. A.; Vetterling, W. T.; Flannery, B. P. *Numerical Recipes in Fortran*, 2nd ed.; Cambridge University Press: Cambridge, 1989.

(18) Bisson, K. Thesis, Université de Paris, Orsay, 1990.

(19) Jørgensen, P.; Swanstrom, P.; Yeager, D. *J. Chem. Phys.* **1983**, *78*, 1347.

(20) It has to be noted that the procedure may have problems. The procedure may generate too large of a shift, the application of which will not lead to much improvement in the energy, or the procedure may result in a step that goes beyond the trust region radius. These problems may be eliminated by enlarging the size of the submatrix and/or reducing the trust region radius. This action has solved these problems in all the cases treated to date. However, since the second-order expansion series is only valid close to the convergence, negative eigenvalues may reflect a lack of chemical intuition from the user (this is also true for CASSCF calculations). Thus, generating well-engineered guess vectors is usually the method of choice. The method has been implemented in order to treat intrinsic problems connected with the optimization of rotations among occupied orbitals and will be discussed in section 3.3.

(21) CASSCF energies and MCSCF energies are not invariant to rotation between doubly occupied inactive orbitals and CI active orbitals. Thus, it is often encountered that swapping a doubly occupied inactive and a CI active would lower the energy. This process manifests itself by a small or negative eigenvalue of the Hessian matrix and consequently a large step in the rotation variable space. With the present method the user can deactivate the rotation that would swap the orbitals and then converge to a meaningful wave function.

(22) Lévy, B. Private communication.

(23) Van Duijneveldt. F. B. IBM Technical Research Report RJ945, 1971.

(24) The total energy of the CASSCF for this calculation is equal to the energy of the full CI calculation in the preoptimized MO basis set and is invariant to the use of symmetry-adapted orbitals or localized orbitals. $E = -40.281\ 595$ au.

(25) Lévy, B. *Chem. Phys. Lett.*, **1973**, *18*, 59.

(26) Veillard, A.; Clementi, E. *Theor. Chim. Acta* **1967**, *7*, 133.

(27) In the full CI calculation, one electronic configuration has 18 unpaired electrons leading to 6770 CSF built with 48 620 Slater determinants whose combined effects are probably negligible.

(28) The double-arrow excitations present particular cases where φ_a and φ_b and/or φ_c and φ_d may be identical.

(29) For an electronic configuration that has 14 unpaired electrons and a spin equal to 0 , only 3432 (number of Slater determinants) numbers of the $2^{14} = 16\ 384$ possible addresses are used. However, the calculation of the address is rapid as it can be realized by bit manipulation. The relative position of one determinant in the list can easily be retreived by one load operation.

(30) Dunning Jr, T. H. *J. Chem. Phys.* **1971**, *55*, 716.

(31) The CASSCF calculation of the $^2\Pi$ state of CH performed with GAMESS-UK does not generate equivalent π_x and π_y orbitals. The distortion energy was evaluated by performing a CASSCF calculation of C_2H_2 at infinite CC distance in which the π_x and π_y orbitals are equivalents. The distortion's energy is equal to 3.4 kcal/mol and is constant for CH distances close to the equilibrium geometry of CH $^2\Pi$ for a 2.15 au CH distance; the $^2\Pi$ total energy of CH is then equal to $-38.313\ 49$ au. However, to compare CASSCF and GMO2, the π_x and π_y orbitals equivalency constraint in GMO2 was removed and inequivalent π_x and π_y orbitals were generated.

(32) Pietsch, M. A.; Couty, M.; Hall, M. B. *J. Phys. Chem.* **1995**, *99*, 16315.